Comparative Study of Bio-implantable Acoustic Generator Architectures

D Christensen, S Roundy

University of Utah, Mechanical Engineering, 50 S. Central Campus Drive, Salt Lake City, UT, USA

E-mail: dave.christensen@utah.edu

Abstract. This paper is a comparative study of the design spaces of two bio-implantable acoustically excited generator architectures: the thickness-stretch-mode circular piezoelectric plate and the bending-mode unimorph piezoelectric diaphragm. The generators are part of an acoustic power transfer system for implanted sensors and medical devices such as glucose monitors, metabolic monitors, drug delivery systems, etc. Our studies indicate that at small sizes the diaphragm architecture outperforms the plate architecture. This paper will present the results of simulation studies and initial experiments that explore the characteristics of the two architectures and compare their performance.

1. Introduction

Advances in sensing and CMOS technology have opened up the possibility of mm scale bio-implantable sensors. However, the size reduction of power and communications technologies (i.e. antennas) has not kept pace with sensing and computation. Therefore, the size of implantable sensors is primarily driven by the power and communications sub-systems. Denisov et. al.[1] have shown that at small sizes and large implant depths acoustic power transmission outperforms electromagnetic power transfer and thus can enable smaller bio-implant sizes.

Two piezoelectric generator architectures that may be employed for acoustic energy transfer are the standard thickness-stretch-mode circular plate (or disk) and the bending-mode unimorph diaphragm. The plate is the more widely used architecture in ultrasonic applications such as imaging and therapy, and seems the more likely candidate for a bio-implantable acoustic generator. On the other hand, the diaphragm seems a mediocre candidate for two reasons. First, it operates in the 3-1 mode which has a much lower coupling coefficient than the 3-3 mode utilized by stretch mode plates. Secondly, diaphragms use significantly less piezoelectric material than plates of the same size and are thus usually outperformed by plates. Prior published works [2][3] have focused on either the plate or diaphragm generator architecture and optimized the generator for a specific application.

2. Model & Experimental Setup

The scaling results of this paper are based on simulation models that include experimental data to evaluate the accuracy of results. The simulation model and experimental setup used are as follows:

2.1. Simulation Model

The simulation models for both architectures are shown in Figure 1. The simulations utilize Mason's network model [4] for the plate and the impedances of the medium. A slightly modified equivalent

network model was used for the diaphragm based on the model proposed by Prasad [2]. In prior published works, the transmitter dynamics have played an important role in the power and efficiency results of the generator [4]. The transmitter dynamics are included in the experimental validation of the model, but are excluded in the scaling simulation. In place of the transmitter is substituted mechanical power into the tissue at 720 mW/cm^2, the maximum safe power input allowed by the United States FDA [5]. This substitution leads to a better comparison and more insightful results.

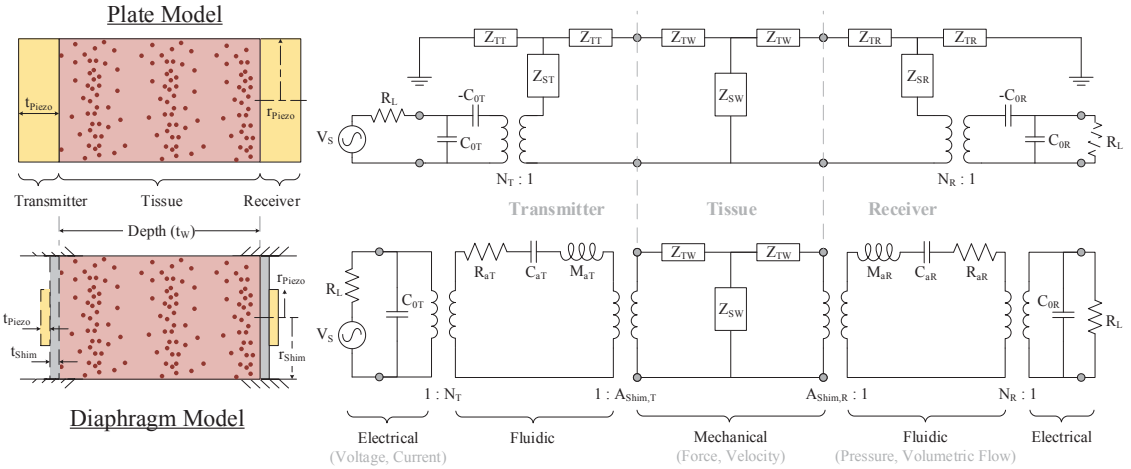

Figure 1. Diagram and simulation model of the plate and diaphragm models.

2.2. Experimental Setup

A tank with adjustable arms was constructed to facilitate testing. Plates (APC Inc., 850 material, 3.43 mm thick, 12.7 mm diameter) and diaphragms (Steminc, SMPD11D11T10F95) were mounted to ABS tubing (McMaster Carr, 1839T371) with cyanoacrylate. All tests were run with a sinusoidal input from a function generator at 2.5 volts amplitude in series with a 100 ohm resistor (R_L = 100 ohms in Figure 1). Plate configurations were given a frequency sweep between 1 Hz and 1 MHz. Diaphragm configurations were given a frequency sweep between 1 Hz and 10 kHz.

3. Results

Experiments with macro-scale devices were run to validate the simulation models. Then scaling simulations were performed to explore the behaviour of the two architectures as dimensions are scaled down to MEMS sizes. First, each transducer was modelled as a stand-alone transmitter. Source current and surface velocity were measured. Damping ratios were experimentally determined. Second, the tested transducers were coupled together and placed in water. A plate transmitter was coupled with a plate receiver and a diaphragm transmitter was coupled with a diaphragm receiver. Transmitter source and receiver generated currents were measured. Lastly, simulations were run to compare the plate and diaphragm architectures at frequencies and diameters of interest. The simulations replace the transmitter with a source intensity and replace water with tissue.

3.1. Transducer Validation

3.1.1. Plate. Figure 2 shows a frequency sweep of the simulated and measured current through the plate transducer. The experimental data shows some lower frequency peaks that are not present in the simulations. These peaks are from the radial vibration mode and harmonics which are not included in the simulation model. The magnitude of the simulated current of the primary extension mode is about 2.2 times greater than the experimentally measured current of the same mode. While the simulated and experimental currents do not match, the simulated and measured velocities of the plate face do match.

This discrepancy of a factor of 2.2 in the source current leads to a mismatch between simulated and measured power output of about a 5 times.

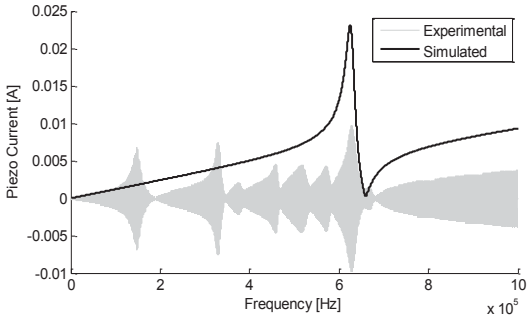

Figure 2. Plate transducer tested as a stand-alone transmitter in air. Simulation results are plotted over experimental data.

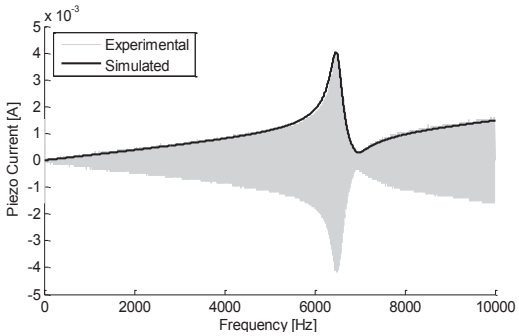

Figure 3. Diaphragm transducer tested as stand-along transmitter in air. Simulation results are plotted over experimental data.

3.1.2. Diaphragm. The diaphragm simulation results closely match the experimental data as shown in Figure 3. While not shown in Figure 3, the velocities measured by the laser vibrometer also indicate a good match. Experimentally measured values of the damping ratio were incorporated into the model.

3.2. Transducers + Medium Validation

3.2.1. Plate. Figure 4 shows simulation and experimental results of the full power transmission model for two plate transducers. The simulation results match the experimental results in expected shape but not magnitude. The magnitudes of both the transmitter and receiver simulation peaks exhibit the 2.2 gain discussed previously.

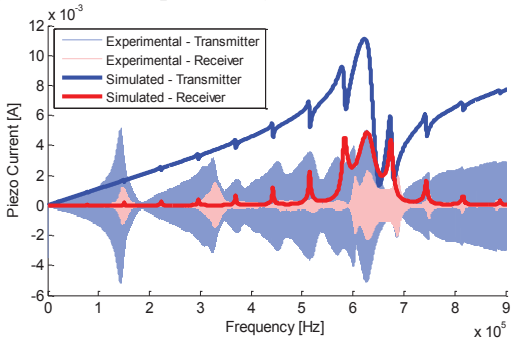

Figure 4. Simulated and measured transmitter and generator current. Plate transmitter and plate receiver separated by 1 cm of water.

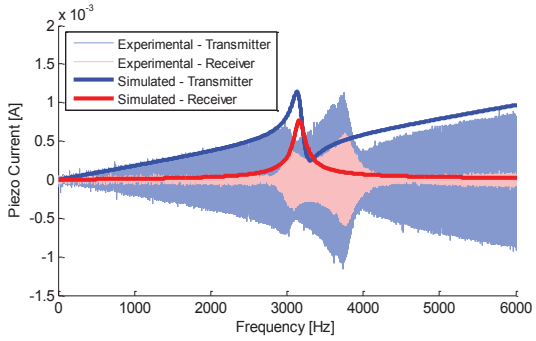

Figure 5. Simulated and measured currents for diaphgram. Diaphragm transmitter and receiver separated by 1 cm of water.

3.2.2. Diaphragm. Figure 5 shows simulation and experimental results of the full power transmission model for two diaphragm transducers. The damping ratio of the diaphragms was found to be much higher in water than in air. Note that the water shifts the resonance of the plate significantly from that measured in air as shown in Figure 5. The models over-estimate this shift.

3.3. Scaled Simulation Comparison

3.3.1. Plate. The scaling simulation of the plate shown in Figure 6 exhibits power loss due to increased absorption at higher frequencies. The diameter to thickness ratio (aspect ratio) is an

important consideration for the model. At aspect ratios lower than 1, the plate becomes a cylinder and the radial mode vibrations play a more significant role in the transducer dynamics. Also, the practical design space for a completed plate device would at least have an aspect ratio of 2 or greater to account for space needed for power electronics, matching layer, and housing. As is clear in Figure 6, it is not practical to design a very small plate generator for low (i.e. 100's of kHz) frequencies where the attenuation in human tissue is lower.

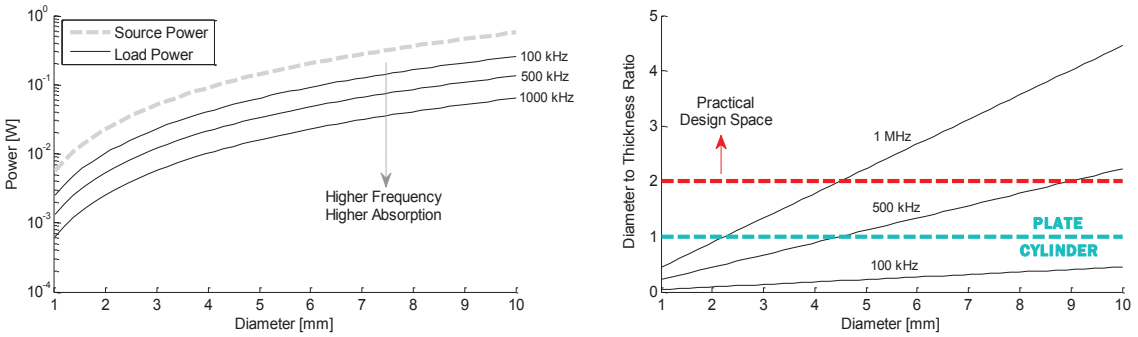

Figure 6. Scaling simulation of the plate architecture at source intensity of 720 mW/cm^2. The optimal plate thickness is ½ the acoustic wavelength, which is determined by the frequency.

3.3.2. Diaphragm. The scaling simulation of the diaphragm shown in Figure 7 exhibits power loss due to increased absorption at higher frequencies like the plate. In the case of the diaphragm, the aspect ratio is important because at low aspect ratios the diaphragm starts to behave more like a plate. At aspect ratios above 10, bending is the significantly dominant strain mode in the diaphragm. At aspect ratios lower than 5, bending strain is insignificant to thickness-stretch strain and a different model would have to be used. Figure 7 indicates that the practical design space for diaphragms is at low ultrasonic frequencies where attenuation is lower and at small diameters which are more desirable for bio-implantable sensors.

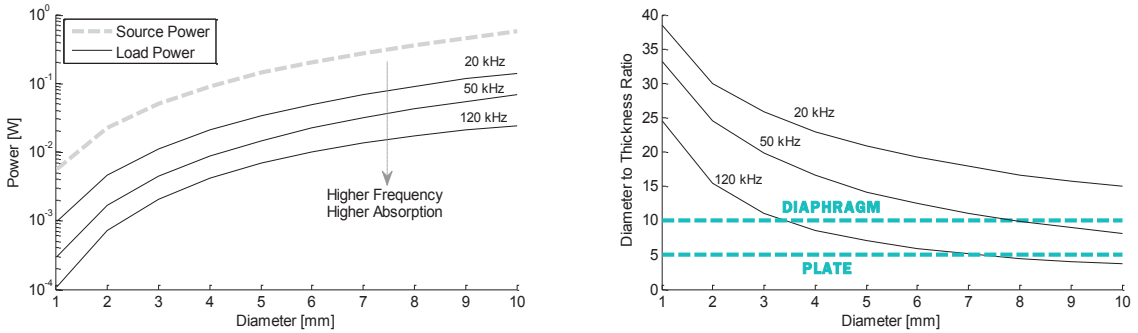

Figure 7. Scaling simulation of the diaphragm architecture at source intensity of 720 mW/cm^2.

3.3.3. Performance Comparison. Combining data from Figure 6 and Figure 7, a direct comparison of the plate and diaphragm is made and shown in Figure 8. The power curves reflect plate architectures with aspect ratios of 2 or greater and diaphragm architectures of 10 or greater. It can be seen that the diaphragm architecture is able to be utilized at lower frequencies with similar efficiency to a larger plate architecture at higher frequencies. The power curves also lead to the not so apparent conclusion that the diaphragm architecture, not the plate, will produce more power for generators of sizes below roughly 5 mm in diameter. Thus, it would be more appropriate for MEMS implementations of ultrasonic bio-implantable sensors.

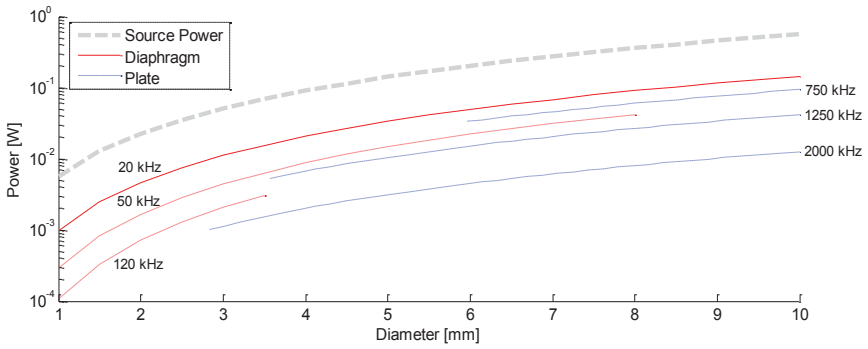

Figure 8. Comparison of plate and diaphragm generators versus diameter for several frequencies at source intensity of 720 mW/cm^2.

4. Discussion

The simulation output shows that the diaphragm will generate more power than the plate at very small sizes (i.e. diameters of 5 mm or less). It should be noted that while the diaphragm model matched the experimental results in terms of power output well, the plate model over-predicted the power output by a factor of approximately 5. Therefore, the plate curves shown in Figure 8 may actually over-predict the power output. This would indicate that at a given size (even up to 9 mm), the comparison may be even more favorable to the diaphragm architecture. However, at larger sizes and lower frequencies, diaphragm displacements may be quite large which could limit their applicability to biological implants.

The ultimate goal of this work is the implementation of a mm scale acoustic power generator capable of producing enough power to operate implantable sensors and communications. On the pathway to this goal, model discrepancies still need to be identified and corrected. This will be followed by ex-vivo tests in tissue or tissue phantoms to demonstrate the power transmission channel and MEMS scale generators.

5. Conclusions

This paper has explored the design space for an acoustically excited generator to power bio-implantable sensors. Two architectures, the standard thickness-stretch-mode plate and a unimorph piezoelectric diaphragm, were evaluated and compared. Simulations and preliminary experimental results indicate that at sizes below roughly 5 mm in diameter the diaphragm architecture is capable of producing more power than the plate.

References

[1] Denisov A and Yeatman E 2010 Ultrasonic vs. Inductive Power Delivery for Miniature Biomedical Implants *2010 International Conference on Body Sensor Networks* (IEEE) pp 84–9

[2] Prasad S A N, Gallas Q, Horowitz S B, Homeijer B D, Sankar B V., Cattafesta L N and Sheplak M 2006 Analytical Electroacoustic Model of a Piezoelectric Composite Circular Plate *AIAA J.* **44** 2311–8

[3] Ozeri S and Shmilovitz D 2010 Ultrasonic transcutaneous energy transfer for powering implanted devices. *Ultrasonics* **50** 556–66

[4] Sherrit S, Badescu M, Bao X, Bar-cohen Y and Chang Z 2005 Efficient Electromechanical Network Models for Wireless Acoustic- Electric Feed-throughs *Proc. SPIE Smart Struct. Conf. San Diego, CA* **5758**

[5] U.S. Department of Health and Human Services 2008 *Guidance for Industry and FDA Staff: Information for Manufacturers Seeking Marketing Clearance of Diagnostic Ultrasound Systems and Transducers*